

# Piezoelectric fields in nitride devices

R. A. Beach and T. C. McGill

*T. J. Watson, Sr. Laboratories of Applied Physics 128-95, California Institute of Technology, Pasadena, California 91125*

(Received 19 January 1999; accepted 3 May 1999)

We have calculated the piezoelectric field and charge distribution for various III-nitride heterostructures. Our calculations include strain energy minimization and doping effects, and are presented to show the magnitude of piezoelectric effects in strained layers. We compare our calculated results to device results where available. These include the two-dimensional electron gas in heterojunction field effect transistors, Schottky diodes with strained layers for Schottky height engineering, and III-nitride single quantum wells. Calculations that included energy considerations resulted in good agreement between predicted and observed field and charge distributions for the heterojunction fields-effect transistors structure. © 1999 American Vacuum Society. [S0734-211X(99)07104-8]

## I. INTRODUCTION

Column III-nitride semiconductors have unique material properties that make them extremely attractive for optoelectronic and high-power, high-frequency applications. Their band gaps range from 1.9 eV for InN to 6.2 eV for AlN. They have small effective masses, typically 0.2 for electrons and 0.5 for holes, and high optical phonon energies in the range of 600–900  $\text{cm}^{-1}$ . In addition they possess a spontaneous electric polarization, and have the largest piezoelectric constants of the semiconductors. This allows for interesting possibilities in strain field engineering. Numerous papers have been published cataloging piezoelectric effects in nitride structures. These include the piezoresistive effect in GaN/AlN/GaN semiconductor–insulator–semiconductor (SIS) structures,<sup>1</sup> in which small deformations of the SIS structure lead to a reduction in the in-plane resistance. A similar effect is seen in AlGaIn/GaN heterojunction field-effect transistors (HFETs). In this case the change in spontaneous polarization and strain induced piezoelectric polarization induce a compensating two-dimensional electron gas (2DEG) at the AlGaIn–GaN interface.<sup>2–4</sup> Piezoelectric fields have also been shown to effect the optical properties of InGaIn/GaN and GaN/AlGaIn quantum wells. The strain induced electric field tilts the conduction and valence bands within the well, resulting in charge separation and increased recombination times as well as a redshift in the emission versus absorption spectrum.<sup>5–7</sup> In the last few years, substantial improvement in the structural and electronic properties of GaN has been achieved. This has resulted in major advances in blue-green light-emitting diodes and lasers as well as HFET power devices. To further improve the performance of these devices, the effects of piezoelectricity must be accounted for. In addition, the use of piezoelectric fields can result in a number of interesting devices such as piezoelectrically enhanced Schottky diodes and photodetectors. We present calculations of the electric fields produced in a number of III-nitride structures. We have used a strain tensor formalism and we compare the results to experiment where available.

## II. BASICS OF PIEZOELECTRICITY

Piezoelectricity is the result of two processes. One is the rearrangement of electronic states in the crystal. The other is displacement of charged constituents within the lattice. Displacement of charged constituents is the dominating process in GaN. A quantitative description of the strain induced polarization is given by

$$P_i = \sum_j e_{ij} \epsilon_j. \quad (1)$$

Here  $P_i$  is the polarization in the  $i$  direction,  $\epsilon_j$  is the  $j$  component of strain, and  $e_{ij}$  is the  $ij$  component of the piezoelectric tensor. The strain generated in pseudomorphic epilayers is determined by the lattice mismatch for the in-plane strain and energy minimization for the perpendicular component of strain. With the three-axis set as the growth direction,  $\epsilon_1$  and  $\epsilon_2$  are given by

$$\epsilon_{1,2} = \frac{a_s - a_l}{a_l}. \quad (2)$$

Here,  $a_s$  ( $a_l$ ) is the substrate (epilayer) lattice constant. The lattice constants were assumed to follow Vegard's law. A recent article by Angerer<sup>8</sup> suggests that Vegard's law underestimates the Al content in hexagonal AlGaIn. This may introduce some slight error in the following analysis, but is unlikely to outweigh the other uncertainties such as Schottky heights of contacts and strain relaxation in epilayers. The strain energy,  $U$ , is given by

$$U = \frac{1}{2} \sum_{ij} C_{ij} \epsilon_i \epsilon_j. \quad (3)$$

The  $C_{ij}$ 's are the elastic constants of the strained layer. The perpendicular component of strain is determined by minimizing this strain energy. The piezoelectric polarization can then be calculated using Eq. (1). For all alloys a linear interpolation of piezoelectric constants and elastic moduli has been used. Due to the lack of experimental data for bulk InN, we have used the elastic coefficients of GaN in place of InN. We have used the spontaneous polarization and piezoelectric constants of Ref. 9, along with the elastic coefficients of

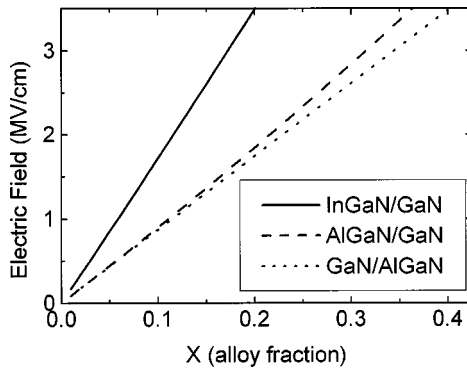


FIG. 1. Comparison of fields in III-N structures

Refs. 10 and 11. The spontaneous polarization of the bulk is assumed to be canceled by charging of surface states. If this were not the case, an enormous field, on the order of a few MV/cm, would be present across the entire sample. The effect of changes in spontaneous polarization from the bulk to epilayer are accounted for in these calculations by assuming a linear relationship between alloy fractions and spontaneous polarizations. Figure 1 shows the calculated fields generated in InGaN/GaN, GaN/AlGaN, and AlGaN/GaN epilayers for undoped structures. The direction of these fields depends on the polarity of the growth. For InGaN grown on GaN and GaN grown on AlGaN, there is a compressive strain in the epilayer. This results in a piezoelectric field in the  $[000-1]$  direction. For AlGaN grown on GaN the strain is tensile, and results in a piezoelectric field in the  $[0001]$  direction. The effect of bulk spontaneous field cancellation is to increase the electric field for GaN/AlGaN and AlGaN/GaN and to decrease the field for InGaN/GaN. It is interesting to note the similarities in electric field for the AlGaN/GaN and GaN/AlGaN structures. From a quick look at the piezoelectric coefficients, one would expect the AlGaN/GaN structure to have a 20% larger field than the GaN/AlGaN structure due to AlN's larger piezoelectric coefficient. This is not the case, however. The change in spontaneous electric field has the same magnitude, but opposite sign, for both structures. Although not shown, the spontaneous contribution represents 2/3 of the resulting field. This results in the closely matched curves for AlGaN/GaN and GaN/AlGaN in Fig. 1. Very good agreement between calculated and observed electric fields was obtained for the GaN/AlGaN structure. For GaN/Al<sub>0.15</sub>Ga<sub>0.85</sub>N a field of 0.46 MV/cm was calculated while measurements employing photoluminescence resulted in a value of 0.42 MV/cm.<sup>6</sup> The electric field is given approximately by  $E = -18.6 \text{ MV/cm} \cdot x (-3.0 \text{ MV/cm} \cdot x)$  for In<sub>x</sub>Ga<sub>(1-x)</sub>N/GaN [GaN/Al<sub>x</sub>Ga<sub>(1-x)</sub>N]. The negative sign indicates an electric field in the  $[000-1]$  direction. This is toward the substrate in metalorganic chemical vapor deposition (MOCVD) and halide vapor phase epitaxy (HVPE) grown samples.<sup>12</sup>

### III. HFETs

Nitride-based HFETs have emerged as attractive candidates for high power devices operating at microwave fre-

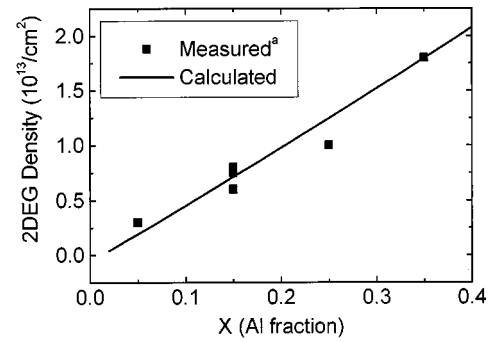


FIG. 2. Comparison of calculated and measured 2DEG densities for AlGaN(300 Å) GaN HFETs. Data from Refs. 4 and 13.

quencies. These devices benefit from a high 2DEG that arises at the AlGaN–GaN interface. This 2DEG has been shown to arise from a large electric field present in the strained AlGaN barrier layer.<sup>3</sup> The expected 2DEG density for a Schottky/AlGaN/GaN structure is given by

$$n_{2d} = \frac{\sigma_p}{e} - \frac{\epsilon_{\text{AlGaN}}}{de^2} (e\varphi_b + E_F - \Delta E_c) + 0.5N_I d. \quad (4)$$

Here,  $\sigma_p$  is the polarization charge at the AlGaN–GaN interface caused by the change in spontaneous polarization and the piezoelectric polarization.  $\epsilon_{\text{AlGaN}}$  is the dielectric constant of the AlGaN layer,  $N_I$  is the doping density in the AlGaN layer, and  $d$  is the AlGaN layer thickness. We have used a value of 1.0 eV for the Schottky barrier height of the contact on GaN. We have assumed an increase in Schottky height for AlGaN identical to the conduction band offset, thus reducing  $e\varphi_b - \Delta E_c$  to  $e\varphi_{\text{GaN}}$ .  $E_F$  is the Fermi level with respect to the conduction band edge at the AlGaN/GaN interface. We have used a value of 0.1 eV for  $E_F$  and  $10^{18}/\text{cm}^3$  for  $N_I$  in these calculations. Figure 2 shows the results of this calculation for variable Al content in the AlGaN layer, and compares the results to experimental measurements found in the literature.<sup>4,13</sup> The thickness of the AlGaN layer is also an important parameter in these HFETs. Figure 3 shows the dependence of the 2DEG density on AlGaN barrier thickness for three Al contents. As can be seen in the figure, a distinct

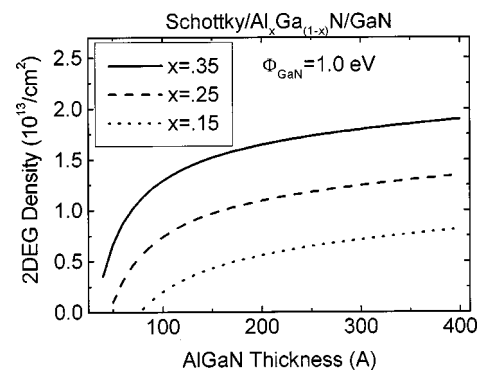


FIG. 3. Thickness dependence of 2DEG in HFETs.

role off occurs in the 2DEG density at  $\sim 150$  Å. After this point, the electron density begins to flatten out with little increase for added thickness.

#### IV. QUANTUM WELLS

Light emitting diodes (LEOs) based on GaN, AlGaIn, and InGaIn have already been produced and marketed with great success.<sup>14</sup> It has been well documented that these quantum well structures possess a large redshift in the emission versus absorption spectrum. This has been shown to result from the piezoelectric fields generated by strain in the well layer.<sup>7</sup> These piezoelectric fields result in charge separation and decreased oscillator strength for the quantum well structure, resulting in decreased efficiency for light emitting devices. Here we incorporate the effects of doping on the fields present in the quantum well, and present a method for determining the most advantageous doping profiles for light emitting devices. Due to the detrimental effects the electric field has on oscillator strength, and hence, quantum efficiency, minimization of these fields is of particular interest to the LED and laser community. Of first order importance is the doping. The polarity of the growth determines the sign of the resulting piezoelectric polarization charge at the well interface. As mentioned earlier, MOCVD and HVPE have been shown to result in Ga faced GaN. This results in a strain generated electric field that points towards the substrate. For the depletion region field to reduce the piezoelectric field a growth sequence resulting in  $p$ -GaIn/InGaIn/ $n$ -GaIn/substrate is required for Ga faced material. For complete cancellation of the electric field in the well region, the charge in the donor depletion region plus the piezoelectric polarization charge at the well-donor region interface must equal zero. A mathematical statement of this is

$$P = qL_d N_d = \sqrt{\frac{2\epsilon_s q N_d N_a V_{bi}}{(N_d + N_a)}}. \quad (5)$$

Here,  $P$  is the polarization in the well,  $N_d$  is the donor density in the  $n$  region,  $N_a$  is the acceptor density in the  $p$  region,  $L_d$  is the depletion length in the donor region,  $\epsilon_s$  is the dielectric constant in the bulk, and  $V_{bi}$  is the built in voltage. Due the high doping concentrations required for  $p$ -type GaIn, a large disparity in doping density occurs in GaIn  $p$ - $n$  structures. Setting the ratio of acceptors in the  $p$  region to donors in the  $n$  region equal to  $\alpha$ , i.e.,  $N_a = \alpha N_d$ , and solving for  $N_d$ , this reduces to

$$N_d = \frac{P^2(\alpha + 1)}{2\epsilon_s q V_{bi} \alpha}. \quad (6)$$

Figure 4 shows the results of this calculation for a range of alloy compositions with  $\alpha$  set to 1. Due to the approximately linear nature of the polarization charge on alloy composition, the doping density can be well approximated by a second order polynomial in  $x$ . For InGaIn/GaIn  $N_d \sim 6.7 \times 10^{20}/\text{cm}^3 x^2$  for GaIn/AlGaIn  $N_d \sim 2.0 \times 10^{19}/\text{cm}^3 x^2$ . These numbers are well within the region of doping densities achieved in GaIn and should not cause difficulties in growth of appropriately doped structures. One caveat that must be

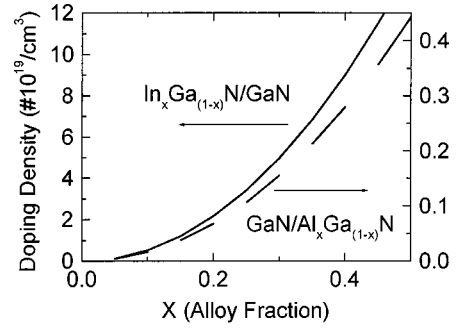


FIG. 4. Graph of required doping density for field cancellation in InGaIn/GaIn and GaIn/AlGaIn quantum wells for  $\alpha$  equal to 1.

discussed is the dependence of the built-in voltage,  $V_{bi}$ , on doping density. The built-in voltage is the energy difference between the fermi levels in the  $n$  and  $p$  layers. We have used a constant  $V_{bi}$  for these calculations of 3.2 eV. This will require modification based on Fermi levels determined for actual devices, but is not expected to vary significantly. In addition, the on state voltage will decrease the depletion region and result in a lower cancellation field. Reduction of the value used here by the voltage drop across the the device in the on state will be required when determining the doping density of the structure.

#### V. SCHOTTKY DETECTORS

Currently, GaIn is predominantly grown with Ga faced polarity.  $N$  faced material, however, can result in a wide range of new and interesting devices. One is a ultraviolet detector employing piezoelectric fields to reject leakage current. Figure 5 shows the structure and band diagram for a field enhanced detector. We present the barrier enhancement and rejection field for this device. A simple electrostatic analysis results in the following equation connecting the Schottky height at the metal-AlGaIn interface to the depletion length in the GaIn bulk.

$$\phi_{\text{AlGaIn}} = \frac{0.5N_d e L^2}{\epsilon_{\text{GaIn}}} + \frac{(N_d e L - \sigma_p) d}{\epsilon_{\text{AlGaIn}}} + \frac{0.5N_1 e d^2}{\epsilon_{\text{AlGaIn}}} + E_F + \Delta E_c. \quad (7)$$

In Eq. (7),  $N_d$  ( $N_1$ ) is the doping density in the GaIn (AlGaIn),  $L$  is the depletion width,  $d$  is the strained layer thickness,  $E_F$  is the Fermi level to conduction band edge energy

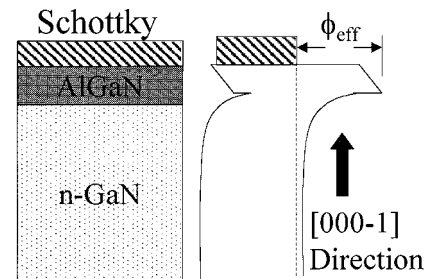


FIG. 5. Schematic of epitaxial layer structure and band-edge energy diagram for Schottky detector.

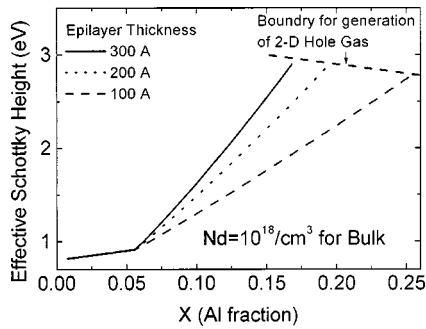


FIG. 6. Graph showing effective Schottky heights as a function of Al mole fraction for three values of epilayer thickness.

separation, and  $\Delta E_c$  is the conduction band offset. After solving this equation for the depletion width ( $L$ ), the effective Schottky height can be calculated from

$$\varphi_{\text{eff}} = \frac{0.5N_d e L^2}{\epsilon_{\text{GaN}}} + E_F + \Delta E_c. \quad (8)$$

Figure 6 shows the calculated effective Schottky height for three values of barrier thickness versus aluminum content in the barrier region. We have used  $10^{18}/\text{cm}^3$  ( $10^{16}/\text{cm}^3$ ) for the bulk (strained layer) doping density.

For low Al mole fraction the barrier height is equal to the Schottky height of the metal-AlGa<sub>N</sub> interface. In this region the polarization field is not large enough to overcome the depletion region field and produce added Schottky height. The Al molar fraction at which this kink occurs is dependent on the doping in the GaN. The maximum effective Schottky height is reached when the GaN valence band at the AlGa<sub>N</sub>/GaN interface moves above the Fermi level. At this point, a 2D hole gas is formed at the AlGa<sub>N</sub>/GaN interface. This is analogous to the electron gas formed in the HFET structure. Increasing the polarization field further results in increased hole accumulation, but little additional height is achieved. It has been found that coherently strained Al<sub>0.25</sub>Ga<sub>0.75</sub>N can be grown up to  $\sim 300$  Å on GaN.<sup>15</sup> This indicates that strain relaxation should not cause a significant shift from these calculated Schottky heights. Doping density is found to have a significant effect on the effective Schottky height. Figure 7

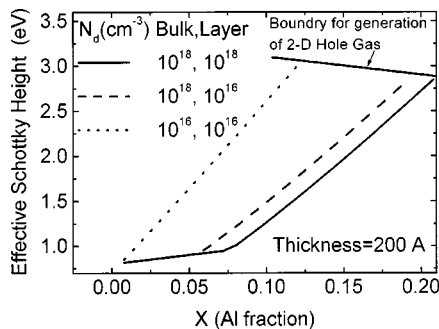


FIG. 7. Effective Schottky height vs Al mole fraction for three sets of doping parameters.

illustrates the changes in effective height with doping in both the barrier layer and bulk. It was found that doping resulted in a later turn on and lower over all enhancement of the Schottky height. Doping in the bulk layer had the greatest effect on Schottky heights, however, doping in the barrier layer caused significant reduction in effective barrier height as well.

## VI. CONCLUSIONS

In summary, we have calculated the piezoelectric fields generated in a few III-nitride structures. These fields were found to be approximately linear with alloy composition and in agreement with experimental photoluminescence measurements. The 2DEG in HFET devices was shown to accumulate quickly after a critical barrier thickness and then level off after approximately 150 Å. It was shown that by the appropriate choice of doping, piezoelectric fields in quantum wells may be reduced or eliminated. The doping densities required for field minimization were shown to be acceptably moderate, and a method for determining the doping density requirements for a given structure was presented. The calculated effective Schottky height for *N*-polar AlGa<sub>N</sub>/GaN photodetectors was presented. The AlGa<sub>N</sub> thickness and Al mole fraction for significant Schottky height increases were found to be moderate and within acceptable growth parameters. Doping was found to decrease the effective Schottky heights in this structure.

## ACKNOWLEDGMENTS

This work has been supported by the Defense Advanced Research Projects Administration and Electric Power Research Institute monitored under ONR Grant No. MDA972-98-1-0005.

- <sup>1</sup>A. D. Bykhovski, V. V. Kaminski, M. S. Shur, Q. C. Chen, and M. A. Khan, *Appl. Phys. Lett.* **68**, 818 (1996).
- <sup>2</sup>A. Bykhovski, B. Gelmont, and M. Shur, *J. Appl. Phys.* **74**, 6734 (1993).
- <sup>3</sup>E. T. Yu, G. J. Sullivan, P. M. Asbeck, C. D. Wang, D. Qiao, and S. S. Lau, *Appl. Phys. Lett.* **71**, 2794 (1997).
- <sup>4</sup>P. M. Asbeck, E. T. Yu, S. S. Lau, G. J. Sullivan, J. Van Hove, and J. Redwing, *Electron. Lett.* **33**, 1230 (1997).
- <sup>5</sup>J. S. Im, H. Kollmer, J. Off, A. Sohmer, F. Scholz, and A. Hangleiter, *Phys. Rev. B* **57**, R9435 (1998).
- <sup>6</sup>J. S. Im, H. Kollmer, J. Off, A. Sohmer, F. Scholz, and A. Hangleiter, *Mater. Res. Soc. Symp. Proc.* **482**, 513 (1998).
- <sup>7</sup>T. Taakeuchi, S. Sota, M. Katsuragawa, M. Komori, H. Takeuchi, H. Amano, and I. Akasaki, *Jpn. J. Appl. Phys., Part 2* **36**, L382 (1997).
- <sup>8</sup>H. Angerer, *Appl. Phys. Lett.* **71**, 1504 (1997).
- <sup>9</sup>F. Bernardini, V. Fiorentini, and D. Vanderbilt, *Phys. Rev. B* **56**, R10024 (1997).
- <sup>10</sup>A. Polian, M. Grimsditch, and I. Grzegory, *J. Appl. Phys.* **79**, 3343 (1996).
- <sup>11</sup>L. E. McNeil, M. Grimsditch, and R. H. French, *J. Am. Ceram. Soc.* **76**, 1132 (1993).
- <sup>12</sup>E. S. Hellman, *MRS Internet J. Nitride Semicond. Res.* **3**, 11 (1998); electronic mail: <http://nrs.mij.mrs.org>
- <sup>13</sup>J. M. Redwing, J. S. Flynn, M. A. Tischler, W. Mitchell, and A. Saxler, *Mater. Res. Soc. Symp. Proc.* **395**, 201 (1996).
- <sup>14</sup>S. Nakamura, M. Senoh, S. Nagahama, N. Iwasa, T. Yamada, T. Matsushita, Y. Sugimoto, and H. Kiyoku, *Appl. Phys. Lett.* **70**, 1417 (1997).
- <sup>15</sup>H. S. Kim, J. Y. Lin, H. X. Jiang, W. W. Chow, A. Botchkarev, and H. Morkoc, *Appl. Phys. Lett.* **73**, 3426 (1998).